Biochemistry

 Volume 39, Number 46 November 21, 2000

Current Topics

Cooperativity and Cooperation in Cyclic Nucleotide-Gated Ion Channels†

Michael J. Richards‡ and Sharona E. Gordon*,‡,§

Department of Ophthalmology and Department of Physiology & Biophysics, University of Washington School of Medicine, Box 356485, Seattle, Washington 98195-6485

Received July 13, 2000; Revised Manuscript Received September 22, 2000

Cyclic nucleotide-gated (CNG)[1] ion channels are nonselective cation channels that are activated by the binding of intracellular cGMP or cAMP (reviewed in ref *1*). The ability to be controlled by these ubiquitous second messengers, to depolarize cells by increasing their Na^+ permeability, and to modulate other cellular systems by changing intracellular Ca^{2+} concentration has made them widely utilized in many types of cells. For example, primary sensory neurons such as photoreceptors and olfactory receptors use CNG channels to transduce stimuli into changes in membrane potential and intracellular Ca^{2+} concentration. Part of what makes CNG channels versatile is the steep dependence of their open probability on cyclic nucleotide concentration. This allows even small changes in cyclic nucleotide concentration to produce large changes in channel activity and thus large changes in membrane conductance. The importance of this class of ion channels is clear when examining the ever-expanding list of tissues in which they are reportedly expressed: heart, lung, kidney, pancreas, liver, spleen, testis, pineal gland, pituitary gland, gustatory epithelium, olfactory epithelium, olfactory bulb, vomeronasal organ, retina, hippocampus, hypothalamus, and cortex (see Table 1). Furthermore, the direct coupling between cyclic nucleotide binding and channel activation, in conjunction with the ability to record transitions in CNG channels with sub-millisecond resolution, makes CNG channels an excellent model system for studying the manner in which agonists drive conformational changes in proteins. This review will begin with an overview of the different CNG channel subfamilies and will discuss the nomenclature that has been used to describe them. We will then examine the functional similarities among CNG channel subfamilies in the context of several classes of models that have been used to describe their activation.

CNG CHANNEL SUBFAMILIES AND NOMENCLATURE

In vivo, CNG channels fall into two basic categories: those that are coupled to cAMP second messenger systems and those that are coupled to cGMP second messenger systems. Despite the various ways that cells utilize CNG channels, similarities and differences among CNG channel subfamilies are not obvious. For example, many of the subfamilies that are activated by cAMP in vivo are better activated by cGMP. In vertebrates, six different CNG channel subfamilies have been identified thus far. As mentioned above, they are widely expressed in neural and nonneural tissue alike (Table 1). Some subfamilies, previously referred to as "α" subunits, form functional cyclic nucleotide-activated channels when expressed exogenously whereas others, previously referred to as "*β*" subunits, do not. The ability to be modulated by calmodulin, to conduct Ca^{2+}, and to interact with other cellular elements also vary from one subfamily to the next. Interestingly, functional properties of subfamilies are not always related to overall sequence homology (*2*). The versatility of CNG channels in cells is expanded by the ability

† This work was supported in part by NIH Grants EY13007 and EY01730 and in part by an unrestricted gift from Research to Prevent Blindness, Inc., New York, NY. S.E.G. is a Jules and Doris Stein RPB Professor.

* Corresponding author. Phone: 206-616-4861. Fax: 206-543-4414. E-mail: seg@u.washington.edu.

‡ Department of Physiology & Biophysics.

§ Department of Ophthalmology.

[1] Abbreviations: cGMP, cyclic 3′,5′-guanosine monophosphate; cAMP, cyclic 3′,5′-adenosine monophosphate; MWC, Monod, Wyman, and Changeux; CD, coupled dimer; HH, Hodgkin Huxley; CNG, cyclic nucleotide-gated.

10.1021/bi001639i CCC: $19.00
Published on Web 10/21/2000

of different subfamilies to coassemble as heteromultimers (*3*). By combining CNG subunits with different properties, a cell can tune channel function to its particular needs. In most cases, combinations of two CNG channel subfamilies are used, but recently a case of three subfamilies forming a functional channel has been reported (*4*).

Since the cloning of the first CNG channel subunit in 1989 (*5*), an explosion of information regarding function, expression, and primary structure has occurred. The number of cloned and sequenced CNG channel subunits has now increased to more than 30. Such a rapid expansion of information inevitably causes confusion with respect to nomenclature. With different nomenclature systems being used by different labs, and some labs (mea culpa) changing the name they use to refer to a particular channel from one paper to the next, it is difficult to communicate which subunit is being referred to without listing several aliases under which it is known. We have therefore compiled a table of CNG channel subfamilies that lists many of their reported names in addition to other relevant information (Table 1).

For this review, we have adopted the nomenclature system of Biel et al. (*6*). CNG1 represents the family which is similar to the so-called α subunit first cloned from rod photoreceptors (*5*), CNG2 represents the family similar to the α subunit cloned from olfactory epithelium (*7*), CNG3 represents the family similar to the α subunit first cloned from cone photoreceptors (*8*), CNG4 represents the family similar to the so-called *β* subunit first cloned from rod photoreceptors (*9, 10*), CNG5 represents the family similar to the *β* subunit first cloned from olfactory epithelium (*11, 12*), and CNG6 represents the family similar to the *β* subunit recently cloned from cone photoreceptors (*13*). We favor this nomenclature system because it is unambiguous and concise. In particular, it omits designations based on function or tissue of expression, which can change with time and cause a name to be outdated and confusing. For the five subfamilies of invertebrate CNG channels, we have used the names they were given when originally published.

EARLY MODELS OF ACTIVATION

How do the 11 subfamilies of CNG channels relate to one another? The sequence identity among subfamilies is quite high, ranging from about 35% to 75%. It is not just in structure, however, that the subfamilies are similar; an examination of their functional properties allows for the formulation of some general rules about CNG channel function. To have a framework for discussing these functional properties, we will review various models that have been used to describe CNG channel activation. This historical perspective will establish a context for focusing on the similarities and differences that distinguish one subfamily from the next.

Before the first CNG channel subunit was cloned, CNG channels were studied primarily in the plasma membranes of rod photoreceptor cells (*14*). These cells have a high density of CNG channels and an absence of other ion channel currents in their outer segments. Using the inside-out configuration of the patch-clamp technique (*15*) from one to several thousand channels could be studied. Furthermore, the concentration of ions on both sides of the membrane, the concentration of cGMP on the cytoplasmic surface, and the presence of other modulatory agents could be tightly controlled. These sorts of experiments shaped our early understanding of the exponential relationship between cGMP concentration and CNG channel open probability.

The first breakthrough in our understanding of CNG channels came from the work of Fesenko et al. (*16*), who applied cGMP to inside-out excised patches from rod outer segments and showed that it directly activates the channels. Analysis of the dose−response relation for activation by cGMP (*16*−*18*) showed that activation of rod outer segment channels, presumably formed from CNG1 and CNG4, is steeply dependent on cGMP concentration, with a limiting slope of about three on a double-logarithmic scale. Interpreting this slope to mean that at least three cGMP molecules must bind to a given CNG channel in order to achieve full activation, Zimmerman and Baylor (*17*) proposed two models to account for this exponential relationship between cGMP concentration and open probability: the independent model and the Hill model. The independent model (Figure 1, top left) specifies one simple way in which cGMP could activate the channels and is essentially the same as that proposed by Hodgkin and Huxley (HH) to account for activation of K^+ channels by voltage (*19*). It presumes that each channel is composed of *n* subunits, each of which can bind cGMP. When cGMP binds to a given subunit, it promotes a conformational change in that subunit. Figure 2 shows data recorded from CNG1 channels expressed in *Xenopus* oocytes (circles). As first shown by Zimmerman and Baylor, the independent model does not adequately fit the cGMP dose−response relation (Figure 2A). In particular, the bend of the predicted dose−response relation is too shallow. The Hill model (Figure 1, top center) assumes that the binding of cGMP to the channel occurs in a highly cooperative manner. As shown in Figure 2B, the measured dose−response relation lies between the curves calculated from the Hill model with the number of subunits (*n*) equal to 2 or 3 (solid curves). Although often requiring noninteger slopes, the Hill equation does provide an adequate empirical description of the dependence of open probability on cyclic nucleotide concentration. The model's ability to empirically describe the data, however, belies the unrealistic nature of its ultimate cooperativity—all the cGMP molecules bind essentially at once.

SEQUENTIAL MODELS OF ACTIVATION

A study that led to the development of a more realistic model for channel activation was conducted by Karpen et al. (*20*). In experiments using a "caged" cGMP that did not activate the channels until instantaneously "uncaged" by a laser flash, Karpen et al. studied the kinetics of channel activation. These experiments, in combination with voltage jump experiments, were used to develop the three-site sequential model of activation. The model proposed that three molecules of cGMP bound to the closed channel and that the fully liganded closed channel then underwent an allosteric conformational change to the open configuration (Figure 1, bottom left). This simple sequential model is more realistic than the Hill model and has only two free parameters: K_T, the equilibrium constant for binding of cGMP to each subunit, and *L*, the equilibrium constant for the allosteric conformational change. At low cGMP concentrations, the channel would occupy mostly unliganded and partially

Table 1: Organization and Nomenclature of the CNG Channel Family Based on Sequence Similarity[a]

subfamily	suggested name	organism	reported names	GenBank Accession No.	clone isolated from	tissue(s) of expression
			Vertebrate Channels			
CNG1 (rod α subunit; rod subunit 1)	btCNG1	*Bos taurus*	bovine rod α (*50*), bovine CNGC1 (*51*), bCNGC1 (*51*), BOVROD (*52*), bRCNC1 (*12*), CNG1 (*53*), brCNGCα (*54*), CNG-1 (*55*), CNCα1 (*4*)	X51604	retina (*5*)	retina (*56*), heart (*57*), kidney (*55*), pineal gland (*58*), adrenal gland (*56*)
	cfCNG1	*Canis familiaris*	dog rod α (*50*), cCNGC1 (*51*)	U83905	retina (*51*)	rod outer segment (*51*), cones (*51*), liver (*51*), kidney (*51*), heart (*51*), brain (*51*)
	ggCNG1	*Gallus gallus*	chicken rod α (*50*), crCNGCα (*58*), rCNG1 (*59*), CCG6 (*8*)	X89599	retina (*8*)	rod outer segment (*8*), pineal organ (*58*)
	hsCNG1	*Homo sapiens*	human rod α (*50*), human CNGC1 (*51*), human rod CNG channel (*60*), hCNGC1 (*51*), hCNG1 (*53*), hRCNC1 (*12*), hrCNGCα (*58*), CNG1 (*61*), hRCNCα (*62*)	NM_000087; M84741; S42457	retina (*63*, *64*)	retina (*63*, *64*), Müller glial cells (*65*), kidney (*61*)
	mmCNG1	*Mus musculus*	mouse rod α (*50*), mRCNC1 (*12*), mIMCD-K2 channel (*66*)	M84742; U19717	retina (*64*), kidney cell line (*66*)	retina (*64*), kidney inner medullary collecting duct (*66*)
	oaCNG1	*Ovis aries*	CNG1 (*67*)	AF067661[c]	kidney (*67*)	not reported
	ocCNG1	*Oryctolagus cuniculus*	rabbit photoreceptor CNGC isoform (*68*)	S65218	SA node region (*68*)	SA node region (*68*), pancreas (*56*)
	rnCNG1	*Rattus norvegicus*	rat rod α (*50*), rat rCNGC1 (*69*), rRCNGC1 (*70*), rCNG (*71*), CNG1 (*61*)	U48803	retina (*69*)	rod outer segment (*69*), ganglion cells (*69*, *71*), bipolar cells (*72*), pineal gland (*73*, *61*), cerebellum (*61*), heart (*61*), spleen (*61*), kidney (*61*, *74*), testis (*61*), lung (*61*), hippocampal neurons (*70*), skeletal muscle (*61*), thalamus (*61*)
	ssCNG1	*Sus scrofa*	PCASM channel (*57*)	U85404	coronary artery smooth muscle (*57*)	coronary artery smooth muscle (*57*)
CNG2 (olfactory α subunit; olfactory subunit 1)	btCNG2	*Bos taurus*	bovine olfactory α (*50*), CNG-2 (*55*), bOCNC1 (*12*), oCNGCα (*72*), BOVOLF (*52*), CNCα3 (*4*)	X55010	olfactory epithelium (*75*)	olfactory neurons (*4*)
	drCNG2	*Danio rerio*	zebrafish olfactory CNG channel (*76*)	U42393[d]	olfactory epithelium (*76*)	olfactory epithelium (*76*)
	ipCNG2	*Ictalurus punctatus*	catfish olfactory α (*50*), fOCNC1 (*12*), oCNGCα (*72*)	M83111	olfactory epithelium (*22*)	olfactory neurons (*22*)
	mmCNG2	*Mus musculus*	mouse olfactory α (*50*), oCNGCα (*72*), oCNC1 (*77*)	U49391	fetal heart (*78*)	heart (*78*), olfactory epithelium (*78*)
	ocCNG2	*Oryctolagus cuniculus*	rabbit aorta α (*50*), rACNG (*79*), CNG-2 (*55*), oCNGCα (*72*)	X59668	aorta (*79*)	heart (*56*), aorta (*56*), brain (*56*), cerebellum (*56*)
	rnCNG2	*Rattus norvegicus*	rat olfactory α (*50*), rOCNC1 (*12*), rOCNGC1 (*70*), CNG2 (*80*), rat oCNGC1 (*69*), CNCα3 (*4*), CNG1 (*81*), rOCNCα (*3*), CNG2 (*61*), CNG-2 (*55*), roCNGCα (*72*)	NM_012928; X55519	olfactory epithelium (*7*)	olfactory neurons (*7*), hippocampal neurons (*70*, *82*), olfactory bulb (*12*, *81*), cerebellum (*12*, *81*), cortex (*12*) pituitary gland (*81*), kidney (*81*)
CNG3 (cone α subunit; cone subunit 1)	btCNG3	*Bos taurus*	bovine cone α (*50*), CNG3 (*61*), BOVCONE (*52*), bovine testis CNG (*60*), CNCα2 (*4*), bcCNGCα (*54*), CNG-3 (*55*), BOVTESTIS (*83*)	X89600; X76485	testis (*83*), kidney (*55*)	pineal organ (*58*), testis (*55*), cones (*83*), heart (*55*), kidney (*55*), retina (*56*), adrenal gland (*56*)

Table 1 (Continued)

subfamily	suggested name	organism	reported names	GenBank Accession No.	clone isolated from	tissue(s) of expression
	ggCNG3	*Gallus gallus*	chick cone α (*50*), CNG3 (*80*), ccCNGCα (*58*)	X89598	retina (*8*)	cone outer segment (*8*), pineal organ (*58*), testis (*58*)
	hsCNG3	*Homo sapiens*	human cone α (*50*), hcCNGCα (*54*), hCCNCα (*3*)	NM_001298	retina (*84*, *54*)	cone photoreceptors (*54*), outer plexiform layer (*54*)
	mmCNG3	*Mus musculus*	CNG3 (*85*)	AJ238239, AJ238240; AJ238241[b]	genomic P1 library(*85*)	cone photoreceptors (*85*)
	rnCNG3	*Rattus norvegicus*	rat g α (*2*), CNGgust (*60*, *86*), CNG3 (*87*)	AF031943;[c,d] AB002801	kidney (*87*), tongue epithelium (*60*, *86*)	kidney (*87*), taste buds (*60*, *86*), cone outer segments (*88*)
CNG4 (rod β subunit; rod modulatory subunit; rod subunit 2)	btCNG4c	*Bos taurus*	bovine rod β (*50*), CNG4c (*89*), CNGβ1c (*90*)	X94707; AF074012	testis (*89*, *90*)	testis (*89*, *90*), retina (*89*)
	btCNG4d	*Bos taurus*	bovine rod β (*50*), CNG4d (*89*)	X94707[e]	testis (*89*)	testis (*89*)
	btCNG4e	*Bos taurus*	bovine rod β (*50*), CNG4e (*89*)	X94707[e]	testis (*89*)	testis (*89*)
	btCNG4f	*Bos taurus*	bovine rod β (*50*), bRCNGCβ (*10*), brCNGCβ (*72*), bCNG4.1 (*59*), CNCβ1a (*4*), CNG4 (*80*), CNG4f (*6*)	X89626	retina (*10*)	retina outer segments (*10*)
	btCNG4k	*Bos taurus*	bovine rod β (*50*), CNGβ1f (*90*)	AF074012[e]	testis (*90*)	testis (*90*), sperm (*90*)
	btCNG4l	*Bos taurus*	bovine rod β (*50*), CNGβ1d (*90*)	AF074013	testis (*90*)	testis (*90*)
	btCNG4m	*Bos taurus*	bovine rod β (*50*), CNGβ1e (*90*)	AF074014	testis (*90*)	testis (*90*)
	hsCNG4a	*Homo sapiens*	human rod β (*50*), hRCNC2a (*9*), hRCNC2 (*12*), CNG4a (*6*), hRCNCβ (*3*)	L15297	retina (*9*)	rod outer segment (*9*)
	hsCNG4b	*Homo sapiens*	human rod β (*50*), CNG4b (*6*), hRCNC2b (*91*), hRCNCβ (*3*)	L15296	retina (*9*)	outer plexiform layer (*9*), rod outer segments (*92*)
	hsCNG4i	*Homo sapiens*	human rod β (*50*), hRCNGCβ (*91*), hCNG4.3 (*59*)	U58837; NM_001297	retina (*62*, *91*, *93*)	rod outer segment (*91*)
	rnCNG4g	*Rattus norvegicus*	rat rod β (*2*), rCNG4.1 (*59*), CNG4g (*6*)	AJ000496	pineal gland (*59*)	pineal gland (*59*)
	rnCNG4h	*Rattus norvegicus*	rat rod β (*2*), CNG4 (*59*), rRCNC2 (*82*), CNCβ1a (*4*), rCNG4.2 (*59*), CNG4h (*6*)	AJ000496[e]	pineal gland (*59*)	pineal gland (*59*), rod photoreceptor (*59*)
	rnCNG4j	*Rattus norvegicus*	rat rod β (*2*), CNG4.3 (*94*), CNCβ1b(*4*)	AJ000515; AF068572	olfactory epithelium (*4*, *94*)	olfactory epithelium (*4*, *94*)
CNG5 (olfactory β subunit; olfactory modulatory subunit; olfactory subunit 2)	rnCNG5	*Rattus norvegicus*	rat olfactory β (*50*), rOCNC2 (*12*, *11*), CNG5 (*80*), CNCα4 (*4*), rOCNCβ (*3*), oCNC2 (*77*)	U12623; U12425	olfactory epithelium (*12*, *11*)	olfactory epithelium (*12*, *11*), brain (*12*), hippocampus (*82*), olfactory bulb (*12*), cerebellum (*12*), cortex (*12*), vomeronasal organ (*77*, *95*)
CNG6 (cone β subunit; cone modulatory subunit; cone subunit 2)	mmCNG6	*Mus musculus*	CNG6 (*13*)	NM_013927; AJ243572	retina (*13*)	inner nuclear layer (*13*), subset of retinal cells (*13*), testis (*13*)
			Invertebrate Channels			
	DmCNGC	*Drosophila melanogaster*	drosophila CNGC1 (*50*), DmCNGC (*52*), DmCNG (*53*), dCNCα (*3*)	X89601	adult head (*52*)	antennae (*52*), eyes (*52*), head fraction (*52*)
	CNGL	*Drosophila melanogaster*	CNGL (*96*)	AB030577	head (*96*)	brain (*96*)
	TAX-4	*Caenorhabditis elegans*	TAX-4 (*97*)	D86922	mixed population worm library (*97*)	sensory neurons (*97*)
	TAX-2	*Caenorhabditis elegans*	TAX-2 (*98*)	U73476	mixed-stage worm library (*98*)	sensory neurons (*98*)
	AtCNGC2	*Arabidopsis thaliana*	AtCNGC2 (*99*)	AF067798; Y16328	plant library CD4−7 (*99*)	not reported
	LCNG1	*Limulus polyphemus*	LCNG1(*53*)	AF091302	brain (*53*)	brain (*53*), ventral eye nerve (*53*)

[a] Commonly used names for subfamilies are reported in parentheses under the subfamily name (in bold). For splice variants, lower case letters are placed after the subfamily number based on the order in which the sequence appeared in the literature. The splice variant lettering for CNG4a−h has been adopted directly from Biel et al. (*6*). Reported name references do not necessarily identify the paper in which the name was originally cited, but the one in which it was used. Multiple GenBank accession numbers represent multiple submissions unless otherwise noted. Reports on the location of CNG channel expression were often unclear and contradictory; thus, no effort was made in judging the veracity of each entry in the "tissue of expression" column. [b] Exons of the coding sequence. [c] GenBank submission only. [d] Only partial sequence reported. [e] Individual splice variant record not provided as sequence can be obtained by a truncation or internal deletion of the reported GenBank record.

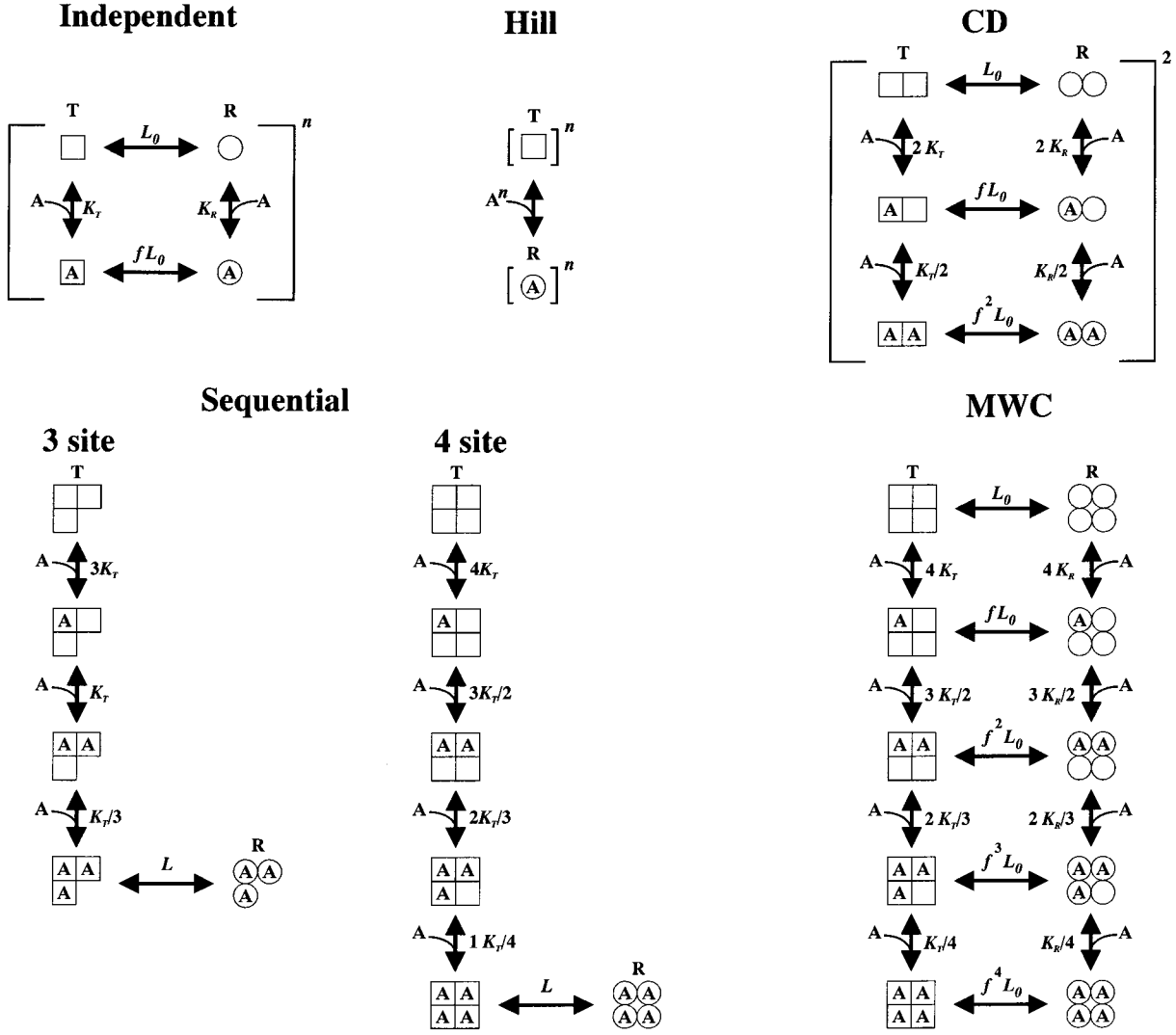

FIGURE 1: Different models that have been used to describe ligand binding and activation in CNG channels. The letter T represents subunits in the inactive (or tense) state, also shown by squares, and the letter R represents subunits in the active (or relaxed) state, also shown as circles. For the Hill model and independent model shown, the superscript *n* represents the number of subunits per channel. For the CD model shown, the superscript 2 reflects the composition of each channel unit of a dimer of dimers. The letter A represents a molecule of agonist, such as cGMP. K_T and K_R are the equilibrium constants for the binding of A to the inactive and active states, respectively, and *f* is equal to K_R/K_T. Modified from Liu et al. (*39*).

liganded states and would therefore be open only a small fraction of the time. Depolarizing the membrane during the voltage jump would do two things: it would change the driving force for permeant ions, and it would make the equilibrium constant *L* more favorable. During the voltage jump experiments typically used to study the channels, these two changes are seen as an instantaneous outward current, produced by the change in ion driving force, and a slower increase in outward current as the equilibrium between closed and open states redistributes the channels closer to the now more favored open state.

With the cloning of the first CNG channel subunit in 1989 (*5*), it was determined that each subunit contained one cGMP binding site. The subsequent elucidation of tetrameric assembly within the voltage-gated superfamily of ion channels (*21*) revealed that a model with only three cyclic nucleotide-binding steps was no longer adequate. The addition of one more cyclic nucleotide-binding step results in a four-site sequential model (Figure 1, bottom center). As can be seen in the solid curves of Figure 2C, both the three- and four-site models produce reasonable approximations of the channel dose−response relation. However, the limiting slope of four predicted by the four-site model is always steeper than that measured for both native channels and exogenously expressed channels and suggests that the sequential model may be too simple to adequately describe channel behavior (see below).

The sequential model for activation has been used to analyze some of the differences between CNG channel subfamilies. With at least one exception (*22*), CNG channels are activated better by cGMP than cAMP regardless of the physiological ligand that activates a given subfamily in vivo (*23*, *24*). In experiments with btCNG1 and rnCNG2 channels expressed exogenously (*25*), two differences were noted between the behavior of cGMP as compared to cAMP: first, cAMP is a full agonist of CNG2 channels but a partial agonist of CNG1 channels, only activating about 1% of the current that can be activated by cGMP; and second, for both cAMP and cGMP, lower concentrations are able to open CNG2 channels as compared to CNG1 channels. These data were interpreted using the sequential model of activation. The model suggested that most of the distinction between

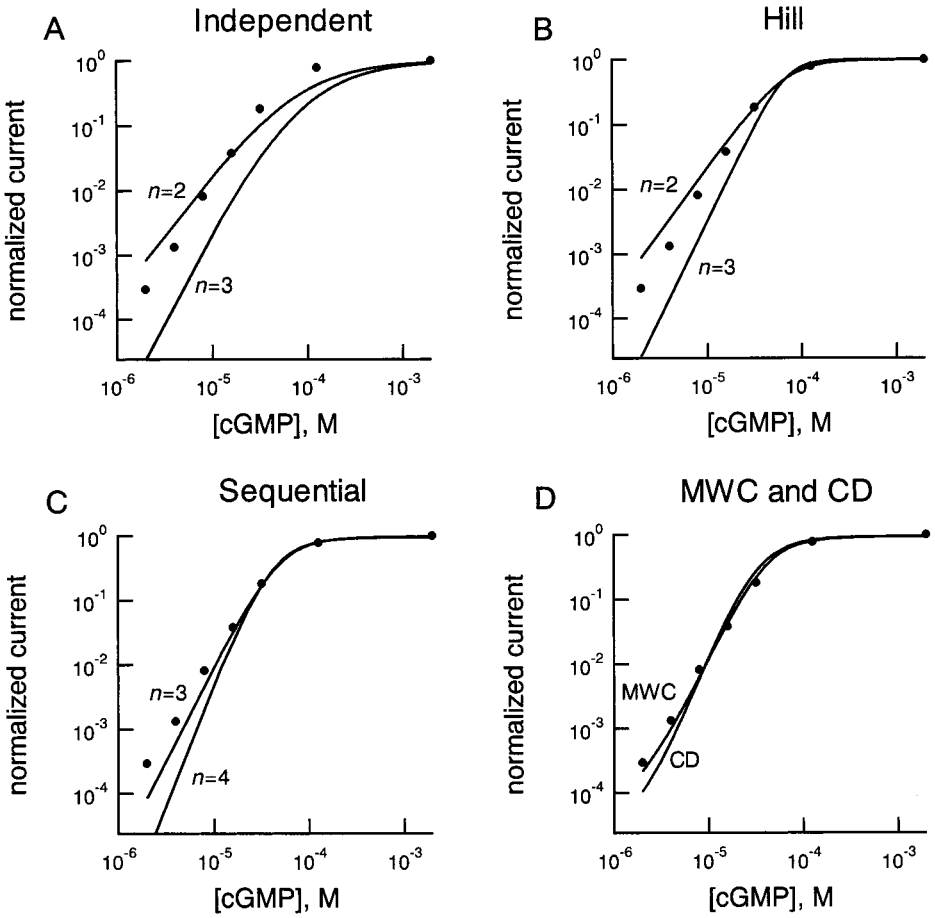

FIGURE 2: Fits of the various models to dose−response data for activation of CNG1 channels by cGMP. The absolute current divided by the current at 2 mM cGMP is plotted on the ordinate, and cGMP concentration is plotted on the abscissa. Data are plotted as circles, and fits using the models from Figure 1 are shown as solid curves, with *n* referring to the number of agonist binding steps required to produce channel activation. The following other parameters were used: (A and B) $K_{1/2} = 67.2\ \mu$M; (C) three-site sequential: $K_T = 6307$, $L = 45$; four-site sequential: $K_T = 13241$, $L = 27$; and (D) MWC: $K_T = 15000$, $L_0 = 1.4 \times 10^{-5}$ (as in ref *32*), $f = 35$; CD: $K_T = 4000$, $L_0 = 0.00374$ (to yield the same unliganded open probability as MWC), $f = 139$.

CNG1 and CNG2 resided in a difference in the equilibrium constant (L) between the fully liganded closed configuration and the fully liganded open configuration. The ratio of L_{cGMP}/L_{cAMP} is comparable for CNG1 and CNG2, but both L_{cGMP} and L_{cAMP} are about 1000-fold lower for CNG1 as compared to CNG2.

Comparing CNG1 and CNG2 using the sequential model thus reveals an interesting difference in their function. Essentially, CNG2 has a lighter "trigger", requiring less cyclic nucleotide in order to produce activation. Furthermore, cAMP is a less effective agonist for both types of channels, so that higher concentrations of it are required, and it is not always able to fully activate the channels even at saturating concentrations. How do the other subfamilies compare in these properties? Those that have been best studied are those that form functional cyclic nucleotide-dependent channels when expressed as homomultimers: CNG1, CNG2, CNG3, DmCNGC, and TAX-4. These subfamilies essentially lie on a spectrum in which the ratio L_{cGMP}/L_{cAMP} is generally constant, while the absolute value of each may change. From more favorable to less favorable, the approximate order is as follows: $L_{TAX-4} > L_{CNG2} > L_{CNG3} \approx L_{DmCNGC} > L_{CNG1}$.

As discussed above, L_{cGMP}/L_{cAMP} is comparable for CNG1, CNG2, CNG3, DmCNGC, and TAX-4 and is a large value reflecting selectivity for cGMP over cAMP. This selectivity is conferred in part by the presence of a negatively charged amino acid in the C-α helix of the cyclic nucleotide-binding domain (D604 in btCNG1) (*26*). A negative charge at this position can interact favorably with the purine ring of cGMP but interacts unfavorably with the purine ring of cAMP. At this same position in CNG4, CNG5, and CNG6, there is a neutral or positively charged amino acid. The neutralization or switching of charge alters the cyclic nucleotide-selectivity causing channels that include CNG4, CNG5, or CNG6 subunits to have increased cAMP selectivity (*11*−*13*, *27*, *28*).

MWC AND CD MODELS OF ACTIVATION

The sequential model of activation proved useful in understanding differences in ligand affinity, ligand efficacy, and functionality between subfamilies. It is not, however, broad enough to serve as a universal model for describing all channel properties. The four-site sequential model predicts a limiting slope of the dose−response relation of four on a double-logarithmic scale whereas the actual dose−response data show a slope of about three for native rod channels (*16*−*18*) and about two for channels expressed exogenously (*5*) (Figure 2). One explanation for the discrepancy between the model and data has been proposed by Ruiz et al. (*29*). They report that the dose−response relation of single CNG1 channels expressed exogenously is steep and highly variable. They suggest that the sum of many such steep and variable

dose−response curves makes the measured macroscopic dose−response relations shallow.

An alternative mechanism that could explain the shallow dose−response relation is one in which opening is not restricted to fully liganded channels. Such a mechanism is exemplified by the Monod, Wyman, and Changeux (MWC)-type model (*30*) (Figure 1, bottom right), which is basically a more elaborate version of the four-site sequential model (*31, 32*). In the MWC model, the channel can open with 0, 1, 2, 3, or 4 cGMP molecules bound, and the binding of each successive cGMP increases the favorability of opening by a factor *f*. The existence of unliganded openings is an important prediction of this model. Such unliganded openings have been observed in expressed CNG channels and occur with a probability in the range of 10^{-4}−10^{-6} (*31, 33, 34*). As shown in Figure 2D, the MWC model can produce a dose−response curve that is shallower than either the four- or the three-site sequential model, and it more closely resembles data from these channels. Furthermore, it has been successfully used to fit data from heteromultimeric channels in which each subunit type had very different cGMP binding profiles or allosteric activation profiles (*32*).

Various different types of models were also tested in experiments in which heteromultimeric channels were created by altering the structure of homomultimeric channels with UV light (*35, 36*). The energy of the flash primarily modified tryptophan residues and produced channels with varying numbers of modified residues per subunit. Since UV modification of tryptophans changes the shape and the maximum of the cGMP dose−response relation, the interdependence between the energetics of activation of a given subunit and the energetics of activation of the channel complex could be examined. Under these conditions, a MWC-type model fit the data well. As expected an independent, HH model, in which binding of cGMP produced an independent conformational change within a given subunit, was not as good at fitting the data.

To fully describe CNG channel behavior, any model must be able to account for subconductance states. Subconductance states are configurations of the channel in which the unitary conductance, the rate at which ions traverse the pore, is decreased. For native rod channels, Taylor and Baylor (*37*) showed a single subconductance state that predominated at low cGMP concentrations. With respect to reconstituted and expressed channels, it is not quite as clear. From zero to as many as four subconductance states have been reported (*34, 38, 39*). However, whether these are related to the sequential binding of four cGMP molecules (*38*) or whether multiple subconductance states can occur with a constant number of cGMP molecules bound per channel (*34*) has not yet been resolved. In principle, the MWC model can easily be expanded to include subconductance states by specifying a unique conductance for each open state or by adding open states with lower conductances. However, the appropriate way to construct such a model will not be clear until consensus is reached on the nature of subconductance states in CNG channels.

An interesting specialization of the MWC model was proposed based on experiments in which wild-type subunits and mutant subunits were co-expressed in the same cell (*39*). When the mutant subunits contained an altered pore sequence, distinct classes of channels could be observed and distinguished by their different unitary conductances. These differing unitary conductances allowed the stoichiometry of wild-type and mutant subunits within a given channel to be determined. Either the wild-type or mutant subunits were then altered by introducing a pair of point mutations into the cGMP binding site, which severely crippled the subunit's ability to bind cGMP. In the presence of a high concentration of cGMP, the number of bound cGMP molecules would equal the number of wild-type cGMP binding sites. Thus, by examining the unitary conductance of a given channel, the number of ligand-bound subunits (i.e., the number with functional cyclic nucleotide-binding domains) and unliganded subunits (i.e., the number with mutant cyclic nucleotide binding domains) could be unambiguously determined. When used to fit the number of functional binding sites versus open probability, the MWC model could not describe the data. Instead, the authors developed a model in which channels were composed of a pair of dimers. In this Coupled Dimer (CD) model, each subunit would bind cGMP in an independent manner, but the two subunits in a dimer would undergo a concerted allosteric conformational change from the closed state to the active state (Figure 1, top right). Each of the two dimers that composed a channel would undergo this conformational change independently, and the channel open probability would be maximal when both dimers were in the active state.

FURTHER EVIDENCE FOR CD MODEL

Evidence supporting a CD-type model also comes from experiments in which the expected 4-fold symmetry of homomultimeric channels has been shown to be broken—at least at the level of particular amino acids or regions. An amino acid, located in the linker region between the last transmembrane domain and the cyclic nucleotide-binding domain (H420 in btCNG1), has been shown to come into close proximity to its mate in an adjacent subunit when channels open (*40*). This pair of histidines then forms a high-affinity Ni^{2+} binding site; when Ni^{2+} is bound, it helps keep these histidines together, thereby potentiating channel activation. Another position three residues away (417 in btCNG1) can also support a histidine−histidine high-affinity Ni^{2+} binding site (*25*). In contrast to the histidines at the 420 position, the histidines at the 417 position bind Ni^{2+} primarily when the channels are closed, inhibiting channel activation. Thus, adjacent subunits "dimerize" in this region with amino acids at the interface of the dimer moving in a state-dependent manner.

Dimerization between adjacent subunits has also been demonstrated at the level of the pore. An acidic residue in the pore of CNG channels forms a binding site for extracellular divalent cations (*41, 42*) as well as the local anesthetic tetracaine (*43*) that blocks from the intracellular surface of the membrane. A glutamic acid at this position in ipCNG2 (363 in btCNG1) has been shown to form a dimer that acts as a binding site for extracellular protons (*44, 45*). One carboxylate group of the glutamic acid from each of two adjacent subunits forms a proton binding site which, when occupied, reduces the unitary conductance of the pore.

In the examples above, deviations from the expected 4-fold symmetry appear to exist in homomultimeric channels, at least at the level of the pore and the region following the

last transmembrane domain. Why would a departure from 4-fold symmetry occur in a protein composed of four identical subunits? Could this departure be related to the heteromultimeric nature of native channels? Native rod, cone, and olfactory channels are composed of at least two types of homologous subunits that contribute to the pore-forming region and contain cyclic nucleotide-binding domains. Recent experiments point to a CNG2−CNG2−CNG5−CNG5 arrangement of subunits for exogenously expressed olfactory channels (*46*) and a CNG1−CNG1−CNG4−CNG4 arrangement of subunits around the central pore of exogenously expressed rod channels (*47*) (however, a CNG1−CNG4−CNG1−CNG4 arrangement for rod channels has also been proposed (*48*)). Furthermore, CNG1 subunits in native rod channels were found to exist as dimers using a protein cross-linking assay (*49*). Thus, an arrangement that favors dimerization in homomultimeric channels may reflect an intrinsic propensity for these channels to form as a pair of unlike dimers in native tissues.

SUMMARY

CNG channels are highly sensitive to changes in cyclic nucleotide concentration. The variety of subfamilies that exist can coassemble to produce channels with a wide range of apparent affinities for cyclic nucleotide and with specificity for either cGMP or cAMP. Efforts to describe channel properties using physical models of channel function have resulted in increased understanding of how these channels work and how the different subfamilies relate to one another. As the number of subunits identified increases and our knowledge of channel function expands, we will be able to form a clearer picture of how these highly evolved cyclic nucleotide sensors perform their roles in a wide array of cell types.

ACKNOWLEDGMENT

We would like to thank Drs. Anita Zimmerman and Bill Zagotta for comments and suggestions and Dr. Steve Siegelbaum for making it easy to use one of his figures.

REFERENCES

1. Zagotta, W. N., and Siegelbaum, S. A. (1996) *Annu. Rev. Neurosci. 19*, 235−63.
2. Wei, J. Y., Roy, D. S., Leconte, L., and Barnstable, C. J. (1998) *Prog. Neurobiol. 56*, 37−64.
3. Finn, J. T., Krautwurst, D., Schroeder, J. E., Chen, T. Y., Reed, R. R., and Yau, K. W. (1998) *Biophys. J. 74*, 1333−45.
4. Bonigk, W., Bradley, J., Muller, F., Sesti, F., Boekhoff, I., Ronnett, G. V., Kaupp, U. B., and Frings, S. (1999) *J. Neurosci. 19*, 5332−47.
5. Kaupp, U. B., Niidome, T., Tanabe, T., Terada, S., Bonigk, W., Stuhmer, W., Cook, N. J., Kangawa, K., Matsuo, H., Hirose, T., Miyata, T., and Numa, S. (1989) *Nature 342*, 762−6.
6. Biel, M., Zong, X., and Hofmann, F. (1996) *Trends Cardiovasc. Med. 6*, 274−80.
7. Dhallan, R. S., Yau, K. W., Schrader, K. A., and Reed, R. R. (1990) *Nature 347*, 184−7.
8. Bonigk, W., Altenhofen, W., Muller, F., Dose, A., Illing, M., Molday, R. S., and Kaupp, U. B. (1993) *Neuron 10*, 865−77.
9. Chen, T. Y., Peng, Y. W., Dhallan, R. S., Ahamed, B., Reed, R. R., and Yau, K. W. (1993) *Nature 362*, 764−7.
10. Korschen, H. G., Illing, M., Selfert, R., Sesti, F., Williams, A., Gotzes, S., Colville, C., Muller, F., Dose, A., Godde, M., Molday, L., Kaupp, U. B., and Molday, R. S. (1995) *Neuron 15*, 627−36.
11. Liman, E. R., and Buck, L. B. (1994) *Neuron 13*, 611−21.
12. Bradley, J., Li, J., Davidson, N., Lester, H. A., and Zinn, K. (1994) *Proc. Natl. Acad. Sci. U.S.A. 91*, 8890−4.
13. Gerstner, A., Zong, X., Hofmann, F., and Biel, M. (2000) *J. Neurosci. 20*, 1324−32.
14. Yau, K. W., and Baylor, D. A. (1989) *Annu. Rev. Neurosci. 12*, 289−327.
15. Hamill, O. P., Marty, A., Neher, E., Sakmann, B., and Sigworth, F. J. (1981) *Pflugers Arch. 391*, 85−100.
16. Fesenko, E. E., Kolesnikov, S. S., and Lyubarsky, A. L. (1985) *Nature 313*, 310−3.
17. Zimmerman, A. L., and Baylor, D. A. (1986) *Nature 321*, 70−2.
18. Haynes, L. W., Kay, A. R., and Yau, K. W. (1986) *Nature 321*, 66−70.
19. Hodgkin, A. L., and Huxley, A. F. (1952) *J. Physiol. 117*, 500−544.
20. Karpen, J. W., Zimmerman, A. L., Stryer, L., and Baylor, D. A. (1988) *Proc. Natl. Acad. Sci. U.S.A. 85*, 1287−91.
21. MacKinnon, R. (1991) *Nature 350*, 232−5.
22. Goulding, E. H., Ngai, J., Kramer, R. H., Colicos, S., Axel, R., Siegelbaum, S. A., and Chess, A. (1992) *Neuron 8*, 45−58.
23. Nakamura, T., and Gold, G. H. (1987) *Nature 325*, 442−4.
24. Furman, R. E., and Tanaka, J. C. (1989) *Biochemistry 28*, 2785−8.
25. Gordon, S. E., and Zagotta, W. N. (1995) *Neuron 14*, 857−64.
26. Varnum, M. D., Black, K. D., and Zagotta, W. N. (1995) *Neuron 15*, 619−25.
27. Fodor, A. A., and Zagotta, W. N. (1996) *Biophys. J. 70*, A368.
28. Gordon, S. E., Oakley, J. C., Varnum, M. D., and Zagotta, W. N. (1996) *Biochemistry 35*, 3994−4001.
29. Ruiz, M., Brown, R. L., He, Y., Haley, T. L., and Karpen, J. W. (1999) *Biochemistry 38*, 10642−8.
30. Monod, J., Wyman, J., and Changeux, J. P. (1965) *J. Mol. Biol. 12*, 88−118.
31. Tibbs, G. R., Goulding, E. H., and Siegelbaum, S. A. (1997) *Nature 386*, 612−5.
32. Varnum, M. D., and Zagotta, W. N. (1996) *Biophys. J. 70*, 2667−79.
33. Picones, A., and Korenbrot, J. I. (1995) *J. Physiol.* (*London*) *485*, 699−714.
34. Ruiz, M. L., and Karpen, J. W. (1997) *Nature 389*, 389−92.
35. Middendorf, T. R., Aldrich, R. W., and Baylor, D. A. (2000) *J. Gen. Physiol. 116* (2), 227−52.
36. Middendorf, T. R., and Aldrich, R. W. (2000) *J. Gen. Physiol. 116* (2), 253−82.
37. Taylor, W. R., and Baylor, D. A. (1995) *J. Physiol.* (*London*) *483*, 567−82.
38. Ildefonse, M., and Bennett, N. (1991) *J. Membr. Biol. 123*, 133−47.
39. Liu, D. T., Tibbs, G. R., Paoletti, P., and Siegelbaum, S. A. (1998) *Neuron 21*, 235−48.
40. Gordon, S. E., and Zagotta, W. N. (1995) *Neuron 14*, 177−83.
41. Root, M. J., and MacKinnon, R. (1993) *Neuron 11*, 459−66.
42. Eismann, E., Muller, F., Heinemann, S. H., and Kaupp, U. B. (1994) *Proc. Natl. Acad. Sci. U.S.A. 91*, 1109−13.
43. Fodor, A. A., Black, K. D., and Zagotta, W. N. (1997) *J. Gen. Physiol. 110*, 591−600.
44. Morrill, J. A., and MacKinnon, R. (1999) *J. Gen. Physiol. 114*, 71−83.
45. Root, M. J., and MacKinnon, R. (1994) *Science 265*, 1852−6.
46. Shapiro, M. S., and Zagotta, W. N. (1998) *Proc. Natl. Acad. Sci. U.S.A. 95*, 14546−51.
47. Shammat, I. M., and Gordon, S. E. (1999) *Neuron 23*, 809−19.

48. He, Y., Ruiz, M., and Karpen, J. W. (2000) *Proc. Natl. Acad. Sci. U.S.A. 97*, 895−900.
49. Schwarzer, A., Schauf, H., and Bauer, P. J. (2000) *J. Biol. Chem. 275*, 13448−54.
50. Zufall, F., Shepherd, G. M., and Barnstable, C. J. (1997) *Curr. Opin. Neurobiol. 7*, 404−12.
51. Zhang, Q., Pearce-Kelling, S., Acland, G. M., Aguirre, G. D., and Ray, K. (1997) *Exp. Eye Res. 65*, 301−9.
52. Baumann, A., Frings, S., Godde, M., Seifert, R., and Kaupp, U. B. (1994) *EMBO J. 13*, 5040−50.
53. Chen, F. H., Ukhanova, M., Thomas, D., Afshar, G., Tanda, S., Battelle, B. A., and Payne, R. (1999) *J. Neurochem. 72*, 461−71.
54. Wissinger, B., Muller, F., Weyand, I., Schuffenhauer, S., Thanos, S., Kaupp, U. B., and Zrenner, E. (1997) *Eur. J. Neurosci. 9*, 2512−21.
55. Biel, M., Zong, X., Distler, M., Bosse, E., Klugbauer, N., Murakami, M., Flockerzi, V., and Hofmann, F. (1994) *Proc. Natl. Acad. Sci. U.S.A. 91*, 3505−9.
56. Distler, M., Biel, M., Flockerzi, V., and Hofmann, F. (1994) *Neuropharmacology 33*, 1275−82.
57. Ratcliffe, C. F., Conley, E. C., and Brammar, W. J. (1995) *Biochem. Soc. Trans. 23*, 441S.
58. Bonigk, W., Muller, F., Middendorff, R., Weyand, I., and Kaupp, U. B. (1996) *J. Neurosci. 16*, 7458−68.
59. Sautter, A., Biel, M., and Hofmann, F. (1997) *Brain Res. Mol. Brain Res. 48*, 171−5.
60. Misaka, T., Kusakabe, Y., Emori, Y., Gonoi, T., Arai, S., and Abe, K. (1997) *J. Biol. Chem. 272*, 22623−9.
61. Ding, C., Potter, E. D., Qiu, W., Coon, S. L., Levine, M. A., and Guggino, S. E. (1997) *Am. J. Physiol. 272*, C1335−44.
62. Grunwald, M. E., Yu, W. P., Yu, H. H., and Yau, K. W. (1998) *J. Biol. Chem. 273*, 9148−57.
63. Dhallan, R. S., Macke, J. P., Eddy, R. L., Shows, T. B., Reed, R. R., Yau, K. W., and Nathans, J. (1992) *J. Neurosci. 12*, 3248−56.
64. Pittler, S. J., Lee, A. K., Altherr, M. R., Howard, T. A., Seldin, M. F., Hurwitz, R. L., Wasmuth, J. J., and Baehr, W. (1992) *J. Biol. Chem. 267*, 6257−62.
65. Kusaka, S., Dabin, I., Barnstable, C. J., and Puro, D. G. (1996) *J. Physiol.* (*London*) *497*, 813−24.
66. Karlson, K. H., Ciampolillo-Bates, F., McCoy, D. E., Kizer, N. L., and Stanton, B. A. (1995) *Biochim. Biophys. Acta 1236*, 197−200.
67. Barley, J., Benjamin, A., Junor, R., and Walters, D. (1998) GenBank.
68. Hundal, S. P., DiFrancesco, D., Mangoni, M., Brammar, W. J., and Conley, E. C. (1993) *Biochem. Soc. Trans. 21*.
69. Barnstable, C. J., and Wei, J. Y. (1995) *J. Mol. Neurosci. 6*, 289−302.
70. Kingston, P. A., Zufall, F., and Barnstable, C. J. (1996) *Proc. Natl. Acad. Sci. U.S.A. 93*, 10440−5.
71. Ahmad, I., Leinders, Z. T., Kocsis, J. D., Shepherd, G. M., Zufall, F., and Barnstable, C. J. (1994) *Neuron 12*, 155−65.
72. Kaupp, U. B. (1995) *Curr. Opin. Neurobiol. 5*, 434−42.
73. Schaad, N. C., Vanecek, J., Rodriguez, I. R., Klein, D. C., Holtzclaw, L., and Russell, J. T. (1995) *Mol. Pharmacol. 47*, 923−33.
74. Ahmad, I., Korbmacher, C., Segal, A. S., Cheung, P., Boulpaep, E. L., and Barnstable, C. J. (1992) *Proc. Natl. Acad. Sci. U.S.A. 89*, 10262−6.
75. Ludwig, J., Margalit, T., Eismann, E., Lancet, D., and Kaupp, U. B. (1990) *FEBS Lett. 270*, 24−9.
76. Barth, A. L., Justice, N. J., and Ngai, J. (1996) *Neuron 16*, 23−34.
77. Berghard, A., Buck, L. B., and Liman, E. R. (1996) *Proc. Natl. Acad. Sci. U.S.A. 93*, 2365−9.
78. Ruiz, M. L., London, B., and Nadal-Ginard, B. (1996) *J. Mol. Cell Cardiol. 28*, 1453−61.
79. Biel, M., Altenhofen, W., Hullin, R., Ludwig, J., Freichel, M., Flockerzi, V., Dascal, N., Kaupp, U. B., and Hofmann, F. (1993) *FEBS Lett. 329*, 134−8.
80. Biel, M., Sautter, A., Ludwig, A., Hofmann, F., and Zong, X. (1998) *Naunyn-Schmiedeberg's Arch. Pharmacol. 358*, 140−4.
81. El-Husseini, A. E.-D., Bladen, C., and Vincent, S. R. (1995) *Neuroreport 6*, 1459−63.
82. Bradley, J., Zhang, Y., Bakin, R., Lester, H. A., Ronnett, G. V., and Zinn, K. (1997) *J. Neurosci. 17*, 1993−2005.
83. Weyand, I., Godde, M., Frings, S., Weiner, J., Muller, F., Altenhofen, W., Hatt, H., and Kaupp, U. B. (1994) *Nature 368*, 859−63.
84. Yu, W. P., Grunwald, M. E., and Yau, K. W. (1996) *FEBS Lett. 393*, 211−5.
85. Biel, M., Seeliger, M., Pfeifer, A., Kohler, K., Gerstner, A., Ludwig, A., Jaissle, G., Fauser, S., Zrenner, E., and Hofmann, F. (1999) *Proc. Natl. Acad. Sci. U.S.A. 96*, 7553−7.
86. Misaka, T., Kusakabe, Y., Emori, Y., Arai, S., and Abe, K. (1998) *Ann. N.Y. Acad. Sci. 855*, 150−9.
87. Qui, W., and Guggino, S. (1997) GenBank.
88. Misaka, T., Ishimaru, Y., Iwabuchi, K., Kusakabe, Y., Arai, S., Emori, Y., and Abe, K. (1999) *Neuroreport 10*, 743−6.
89. Biel, M., Zong, X., Ludwig, A., Sautter, A., and Hofmann, F. (1996) *J. Biol. Chem. 271*, 6349−55.
90. Wiesner, B., Weiner, J., Middendorff, R., Hagen, V., Kaupp, U. B., and Weyand, I. (1998) *J. Cell Biol. 142*, 473−84.
91. Colville, C. A., and Molday, R. S. (1996) *J. Biol. Chem. 271*, 32968−74.
92. Chen, T. Y., Illing, M., Molday, L. L., Hsu, Y. T., Yau, K. W., and Molday, R. S. (1994) *Proc. Natl. Acad. Sci. U.S.A. 91*, 11757−61.
93. Ardell, M. D., Aragon, I., Oliveira, L., Porche, G. E., Burke, E., and Pittler, S. J. (1996) *FEBS Lett. 389*, 213−8.
94. Sautter, A., Zong, X., Hofmann, F., and Biel, M. (1998) *Proc. Natl. Acad. Sci. U.S.A. 95*, 4696−701.
95. Broillet, M. C., and Firestein, S. (1997) *Neuron 18*, 951−8.
96. Miyazu, M., Tanimura, T., and Sokabe, M. (2000) *Insect. Mol. Biol. 9*, 283−92.
97. Komatsu, H., Mori, I., Rhee, J. S., Akaike, N., and Ohshima, Y. (1996) *Neuron 17*, 707−18.
98. Coburn, C. M., and Bargmann, C. I. (1996) *Neuron 17*, 695−706.
99. Leng, Q., Mercier, R. W., Yao, W., and Berkowitz, G. A. (1999) *Plant Physiol. 121*, 753−61.

BI001639I